Environ. Sci. Technol. **2008,** *42,* 5137–5143

Transitional Adsorption and Partition of Nonpolar and Polar Aromatic Contaminants by Biochars of Pine Needles with Different Pyrolytic Temperatures

BAOLIANG CHEN,* DANDAN ZHOU, AND LIZHONG ZHU

Department of Environmental Science, Zhejiang University, Hangzhou, Zhejiang 310028, China

Received January 29, 2008. Revised manuscript received May 3, 2008. Accepted May 5, 2008.

The combined adsorption and partition effects of biochars with varying fractions of noncarbonized organic matter have not been clearly defined. Biochars, produced by pyrolysis of pine needles at different temperatures (100−700 °C, referred as P100−P700), were characterized by elemental analysis, BET-N_2 surface areas and FTIR. Sorption isotherms of naphthalene, nitrobenzene, and *m*-dinitrobenzene from water to the biochars were compared. Sorption parameters (N and $\log K_f$) are linearly related to sorbent aromaticities, which increase with the pyrolytic temperature. Sorption mechanisms of biochars are evolved from partitioning-dominant at low pyrolytic temperatures to adsorption-dominant at higher pyrolytic temperatures. The quantitative contributions of adsorption and partition are determined by the relative carbonized and noncarbonized fractions and their surface and bulk properties. The partition of P100−P300 biochars originates from an amorphous aliphatic fraction, which is enhanced with a reduction of the substrate polarity; for P400−P600, the partition occurs with a condensed aromatic core that diminishes with a further reduction of the polarity. Simultaneously, the adsorption component exhibits a transition from a polarity-selective (P200−P400) to a porosity-selective (P500−P600) process, and displays no selectivity with P700 and AC in which the adsorptive saturation capacities are comparable to predicted values based on the monolayer surface coverage of molecule.

Introduction

Environmental black carbons (BCs), such as chars and soots, are widely found in soil, sediment, and aerosols (*1*–*5*). Quantification and characterization of environmental BCs in sorption of neutral organic contaminants (NOCs) have been pursued by many investigators (*1*–*3*, *6*–*14*). Environmental BCs stem mainly from the incomplete combustion of biomass and fossil fuel (*1, 2, 4, 5*). The burning of vegetation is usually the primary cause of char formation in forest and agricultural soils (*9*). To investigate the sorptive behavior of the BC, some surrogate materials such as wood charcoals and crop residue-derived chars have been prepared under various conditions and tested (*3, 7, 9*–*14*).

* Corresponding author phone: 0086-571-8827-3901; fax: 0086-571-8827-3693; e-mail: blchen@zju.edu.cn.

The biochar (biomass-derived black carbon) is a ubiquitous form of black carbon in soils capable of sequestering other substances in terrestrial ecosystems (*1, 2, 15*–*18*) because of its recalcitrance to decomposition and mineralization (*15*). This sequestering ability of a biochar depends strongly on its properties, which are influenced in turn by their pyrolytic condition. Application of biochars to soil may enhance the sequestration of atmospheric carbon dioxide (*15*–*18*) and improve the soil fertility for crop production (*9, 17, 18*). Addition of BC-containing ashes to soil is found to enhance the *adsorptivity* of the soil for pesticides (*9*). However, the combined adsorption and partition effects of biochars with varying fractions of noncarbonized organic matter have not been clearly defined.

Most BCs or biochars are not fully carbonized (*3, 10, 12*). The carbonized organic matter (COM) is expected to behave as an adsorbent and the noncarbonized organic matter (NOM) as a partition (absorption) phase (*12, 19, 20*); adsorption is typically nonlinear, whereas partition is essentially linear (*2, 19, 20*). In this sense, the sorptive uptakes of biochars are determined by the relative carbonized and noncarbonized fractions and their surface and bulk properties. It has been observed that the sorption of NOCs to crop-residue chars produced at low pyrolytic temperatures results from both adsorption with COM and partition with NOM, whereas the sorption to same high-temperature chars occurs mainly by adsorption (*12*). The adsorption of aromatic hydrocarbons to a natural wood char is assisted by π-electron interactions (*13*) and proceeds with a pore-filling mechanism (*7*).

The primary objective of this study is to demonstrate the hypotheses that the relative contributions of adsorption with COM and partition with NOM of biochars are quantitatively regulated by the transitional compositions of the biochar with different pyrolytic temperature. Toward this end, a series of biochars were produced by the pyrolysis of pine needles, a model for the forest litter, under a wide range of temperatures (100−700 °C). The samples were characterized via elemental analysis, BET-N_2 surface area, and Fourier transform infrared spectroscopy (FTIR). Sorption isotherms of nonpolar (naphthalene) and polar (nitrobenzene and *m*-dinitrobenzene) aromatic compounds on eight biochars and a commercial activated carbon from water were compared. Partition and adsorption effects were quantified via an isotherm-separation method, with the results evaluated with respect to biochar compositions. In light that pine needles used for biochars form a common litter in forests and are highly flammable, the chars thus derived may serve as a useful reference to those in some forests produced by fire, and their sorption behaviors will further enrich sorption of forest BC.

Materials and Methods

Biochar Samples. Biochars were produced via pyrolyzing biomass at various temperatures under oxygen-limited conditions. Dry pine needle litters were collected and washed with tap water four times to remove dusts. After air-dried for 2 days and subsequently oven-dried overnight at 70−80 °C, the litters were ground and then passed through a 0.154 mm sieve. The preparation procedure was modified from a previous procedure (*12*), which restricts the oxygen supply to the biomass and thereby allows the material to be charred rather than combusted. In brief, the needle powder (20 g) was placed in a ceramic pot, covered with a fitting lid, and pyrolyzed under the oxygen-limited conditions for 6 h under a wide range of temperatures (i.e., 100, 200, 250, 300, 400, 500, 600, and 700 °C). The resulting charred residues were pulverized for subsequent demineralization with acids. The

10.1021/es8002684 CCC: $40.75
Published on Web 06/11/2008

TABLE 1. Yields, Elemental Compositions, Atomic Ratios, Ash Contents, BET-N_2 Specific Surface Area (SA), and Total Pore Volume (TPV) of the Bio-Chars Prepared under Different Temperatures and a Commercial Activated Carbon (AC) [a]

sample	temp/°C	yield/%	C/ %	H/ %	N/ %	O/ %	(O+N)/C	O/C	H/C	Ash/%	SA/$m^2 \cdot g^{-1}$	TPV/ $mL \cdot g^{-1}$
P100	100	91.2 ± 0.6	50.87	6.15	0.71	42.27	0.635	0.623	1.440	1.05	0.65	
P200	200	75.3 ± 0.4	57.10	5.71	0.88	36.31	0.490	0.477	1.191	0.90	6.22	
P250	250	56.1 ± 1.0	61.24	5.54	0.86	32.36	0.408	0.396	1.077	1.24	9.52	
P300	300	48.6 ± 1.2	68.87	4.31	1.08	25.74	0.294	0.280	0.746	1.91	19.92	
P400	400	30.0 ± 1.2	77.85	2.95	1.16	18.04	0.187	0.174	0.451	2.32	112.4	0.0442
P500	500	26.1 ± 0.5	81.67	2.26	1.11	14.96	0.149	0.137	0.329	2.80	236.4	0.0952
P600	600	20.4 ± 1.0	85.36	1.85	0.98	11.81	0.114	0.104	0.258	2.76	206.7	0.0764
P700	700	14.0 ± 0.5	86.51	1.28	1.13	11.08	0.107	0.096	0.176	2.20	490.8	0.186
AC			79.79	1.72	0.67	17.82	0.175	0.168	0.256	0.76	1036	0.434

[a] Elemental compositions and atomic ratios are on an ash-free basis. H/C: atomic ratio of hydrogen to carbon. O/C: atomic ratio of oxygen to carbon. (O+N)/C: atomic ratio of sum of nitrogen and oxygen to carbon.

samples were treated in 200 mL of 1 mol/L HCl solution for 12 h and centrifuged to remove the supernatants. The residues were rinsed with deionized distilled water until the aqueous phase became neutral. The char samples were then oven-dried overnight at 70−80 °C. The biochar samples are hereafter referred to as P100, P200, P250, P300, P400, P500, P600, and P700, respectively, where the suffix number to chars represents the pyrolytic temperature. The yields of each biochar were recorded in Table 1. Since the char contains noncarbonized matter, the term *biochar* was used instead of *charcoal*. For comparison, an analytical-grade powder activated carbon (AC, Shanghai Chemical Co. Ltd.), passed through a 0.154 mm sieve, was selected as a reference for a fully carbonized adsorbent.

Characterization of Samples. Elemental (C, H, N) analyses were conducted using an EA 112 CHN elemental analyzer (Thermo Finnigan). The oxygen content was determined by a mass balance. The H/C and (O+N)/C atomic ratios were calculated to evaluate the aromaticity and polarity, respectively, of the biochar. Ash content was measured by heating the samples at 800 °C for 4 h. FTIR spectra were recorded in the 4000−400 cm^{-1} region by a Nicolet FTIR spectrophotometer (model 560) with a resolution of 4.0 cm^{-1}. The surface areas were measured with N_2 (0.162 nm^2) adsorption at liquid nitrogen temperature determined by a NOVA-2000E surface area analyzer. Four data points, with relative pressures of 0.05 to 0.3, were used to construct the monolayer adsorption capacity. The total pore volume was estimated from a single-N_2 adsorbed point at a relative pressure of about 0.99.

Batch Sorption Experiment. Naphthalene (NAPH), nitrobenzene (NB), and *m*-dinitrobenzene (*m*-DNB) were chosen as model sorbates due to their different molecular polarities and dimensions. Their physicochemical properties and dimensions are shown in Supporting Information Table S-1 and Figure S-1, respectively. All sorption isotherms were obtained in 0.01 mol/L $CaCl_2$ to simulate environmental water, with 200 mg/L NaN_3 added to inhibit the degradation by incidental bacteria. Relative initial concentrations (C_i/C_S) ranged from 0.03 to 0.94 for NAPH, 0.01 to 0.83 for NB, and 0.02 to 0.87 for *m*-DNB to saturate potential adsorption. The solid-to-water ratios are detailed in the Supporting Information. Isotherms consisted of 10 concentration points; each point, including the blank and calibration control, was run in duplicate. The vials were placed on a rotating shaker and agitated in the dark at 20 rpm for 3 days. Preliminary tests indicated that apparent equilibrium was achieved in less than 48 h (see Supporting Information Figure S-2), which is consistent with previously kinetic studies about wood and crop chars (ref *12* and references therein). The solution was separated from solids by centrifugation at 4000 rpm for 15 min. The equilibrium concentrations were measured by using a UV-2550 spectrophotometer (see the Supporting Information). Because of a minimal sorption by the vials and no biodegradation observed, the amount sorbed by sorbent was calculated by the sorbate mass difference in solution.

Results and Discussion

Characteristics of Biochars. FTIR spectra of biochars (P100−P700) and their spectroscopic assignment are shown in Figure 1. For P100 biochar, the band at 3400 cm^{-1} represents the stretching vibration of hydroxyl groups. The bands at 2927, 2856, 1446, and 1370 cm^{-1} are assigned mainly to CH_2 units in biopolymers (*21*). The peaks at 1734 and 1160 cm^{-1} are assigned to C═O and C−O stretching vibrations of ester bonds, respectively. The band due to aliphatic C−O−C and alcohol-OH (1160−1030 cm^{-1}) represents oxygenated functional groups of cellulose (*22*). The band at 1613 cm^{-1} is assigned to C═C and C═O stretching in the aromatic ring (*12, 13, 22*), and the peak at 1514 cm^{-1} represents the C═C ring stretching vibration of lignin (*22*). The band at 1270 cm^{-1} is assigned to the aromatic CO− and phenolic −OH stretching (*12*). The peak of 815 cm^{-1} is assigned to the aromatic CH out-of-plane deformation. All these bands experience different changes with increasing pyrolytic temperature. At low pyrolytic temperatures (100 → 250 °C), the band intensities at 3400 cm^{-1} (−OH) and 1160−1030 cm^{-1} (C−O) are dramatically decreased, whereas other bands (e.g., $-CH_2-$, C═C, and ester C═O) are preserved. The polar groups (−OH and C−O) are significantly eliminated upon heating at low temperature and exhibited the largest loss (Table 1). The band intensities for aromatic CO− and phenolic −OH groups (1270 cm^{-1}) decrease when heating to 300 °C. The ester C═O peaks (1734 and 1160 cm^{-1}) diminished at 300 °C and is completely eliminated when heating to 500 °C. The intense bands for aliphatic CH_2 (2927, 2856, and 1446 cm^{-1}) disappear abruptly when heating to 400 °C, indicating a decrease of the nonpolar group contents. The intensity of the band at 1613 cm^{-1} (aromatic C═C and C═O) remained largely unchanged between 100 and 400 °C, diminished at 500−700 °C (*12*). The sharp peaks at 1145−1100 cm^{-1} for P700 and AC are assigned to C−O and C–C stretching. Due to thermal destruction of cellulose, ester C═O, aliphatic alkyl, and aromatic C═O and −OH groups, the aromatic cores derived from lignin fractions are exposed and remained at high charring temperatures.

The elemental compositions and surface area in Table 1 are in line with the observations of FTIR. With increasing pyrolytic temperature, the carbon content increased, whereas the oxygen and hydrogen contents decreased. The observed H/C ratio sharply decreased. The H/C of 0.176 for P700 indicates that the biochar is highly carbonized and exhibits a highly aromatic structure (*12*). On the other hand, the much higher H/C ratio for P100, P200, and P250 (H/C ratio >1.0) suggests that these biochars contain a good amount of original organic residues, such as polymeric CH_2 and fatty acid, lignin (aromatic core), and some cellulose (polar fractions). As

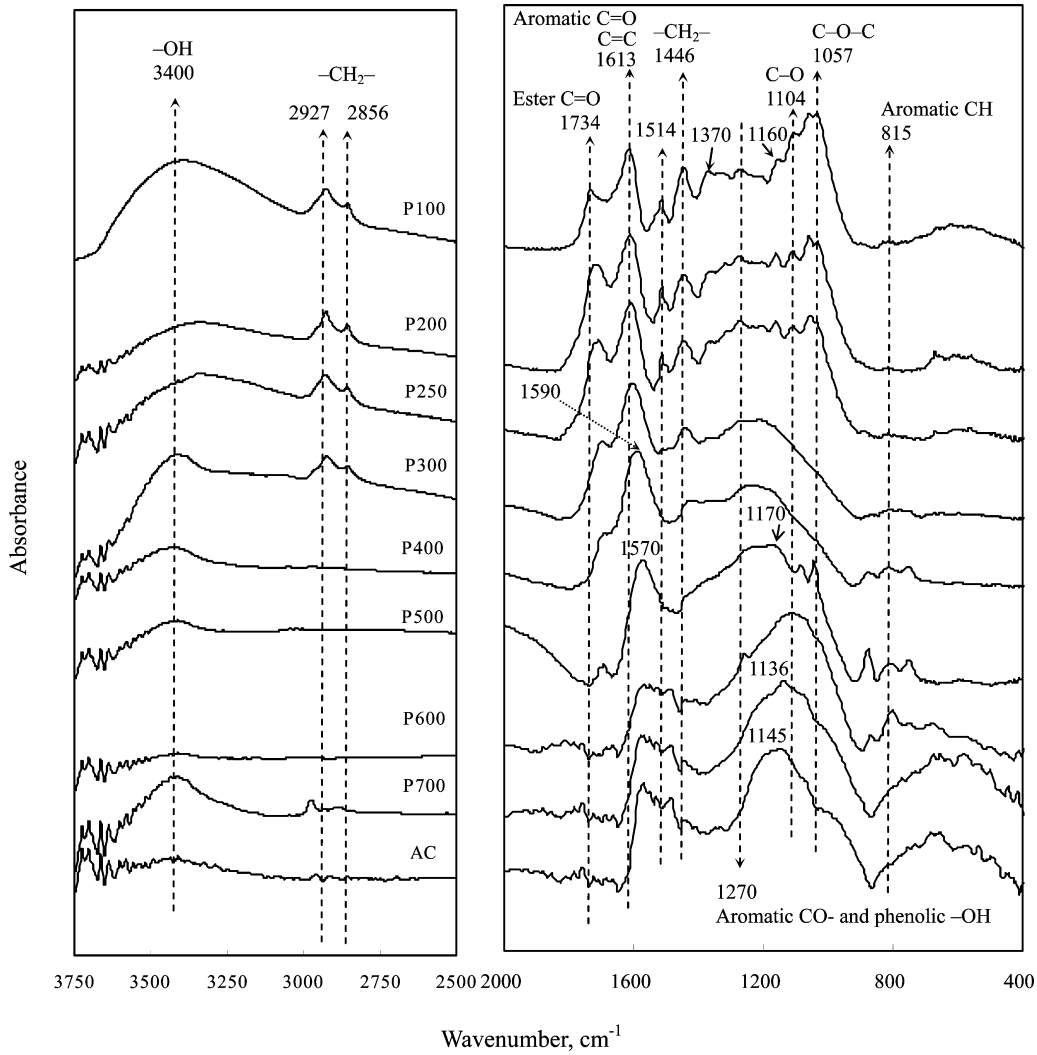

FIGURE 1. FTIR spectra of the biochars (P100−P700) and an activated carbon sample.

shown in Table 1, the molar O/C ratio decreases with increasing pyrolytic temperature, such that the surfaces of high-temperature biochars become less hydrophilic (*1, 12*). The decrease of the polarity index [(O+N)/C] with the pyrolytic temperature indicates a reduction of the surface polar functional groups.

The surface area (SA) of P100 is extremely low (0.65 m^2/g, Table 1). With increasing pyrolytic temperature (100 → 300 °C), the removal of −OH, aliphatic C−O and ester C=O groups from outer surfaces of pine needles resulted in a slow enhancement of SA of P200 (6.22 m^2/g), P250 (9.52), and P300 (19.92). Interestingly, the SA of P400 jumped sharply to 112.4 m^2/g due to the complete destruction of aliphatic alkyl and ester C=O groups shielding the aromatic core. The further removal of aromatic CO− and phenolic −OH linked to aromatic cores at high pyrolytic temperature greatly enlarges the SA of biochars. The high SAs of P500, P600, and P700 (>200 m^2/g) suggest that these samples possess some fine-pore structures. The SA and total pore volumes (TPV) of the biochars are significantly lower than the commercial activated carbon (SA = 1036 m^2/g and TPV = 0.434) due to the latter experiencing further activation process (*12*). Note that a reduction in SA and pore volume above a certain temperature was observed (*11, 12*). Major changes in structures of biochars, regulated by the pyrolytic temperature, would have huge impacts on their adsorptive and absorptive (partition) effects with NOCs.

Sorption of Organic Contaminants onto Biochars. Sorption of NAPH, NB and *m*-DNB onto P100−P700 and AC were investigated, presented in Figure 2 (NB) and Supporting Information Figure S-3 (NAPH and *m*-DNB). The isotherms fit the Freundlich equation, with the related parameters listed in Supporting Information Table S-2. The isotherms of all solutes on P100 are practically linear, with respective Freundlich $N = 1.107 \pm 0.021$, 0.971 ± 0.019, 0.983 ± 0.016 for NAPH, NB, and *m*-DNB, suggesting that the partitioning into the P100 noncarbonized organic matter (NOM) is the dominant mechanism.

The isotherms for P200−P700 display an increasing nonlinearity (*N* index, Supporting Information Table S-2) of a concave-downward curvature at low solute concentrations but exhibit a practically linear shape at moderate to high concentrations (C_e/C_s = 0.1−0.7). Similar results were observed for sorption by soils of polar and nonpolar organic solutes from water over a wide range of C_e/C_s (the ratio of equilibrium concentration to aqueous solubility) (*19*). The nonlinearity at low C_e/C_s is attributed to a significant solute adsorption on a small amount of a high-surface area carbonaceous material (HSACM, e.g., a charcoal-like substance) in soil and to a specific interaction of a polar solute with highly active NOM sites. At moderate to high C_e/C_s, this adsorption becomes largely saturated and the partition in NOM predominates to give an essentially linear isotherm. In the present study, the curvature at low C_e/C_s with biochars increases with the pyrolytic temperature (200 → 700 °C), due presumably to increased carbonization of NOM to produce charcoal-like materials (*12*). For P200, P250, and P300, the observed small nonlinearity at low C_e/C_s and essential

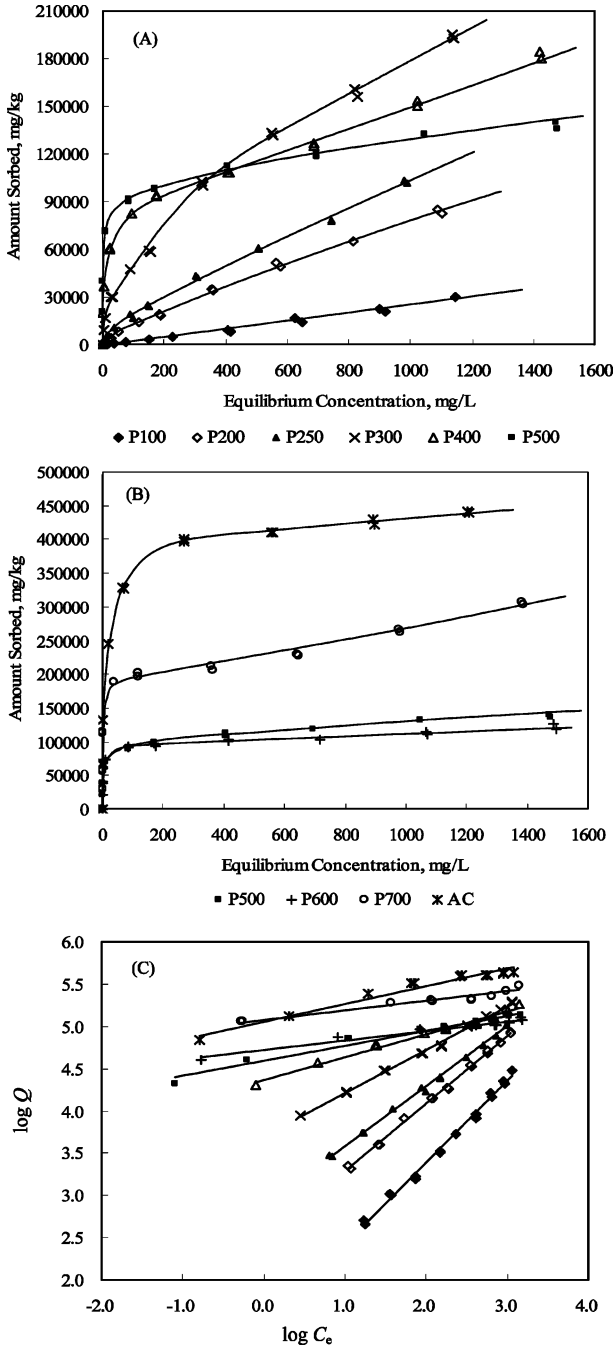

FIGURE 2. Sorption isotherms of nitrobenzene to the biochars (P100−P700) and an activated carbon (AC) sample in aqueous solution.

linearity at high C_e/C_s are reflective of a large amount of low-SA amorphous moiety in biochars. For P400, P500, P600, and P700, highly nonlinear isotherms ($N < 0.4$) occur, reflecting a large amount of HSACM being formed. Consequently, the Freundlich N values exhibit a transition from 0.8∼0.7 (low nonlinear) to 0.5∼0.4 (moderately nonlinear), then to 0.1∼0.2 (highly nonlinear), with a concomitant increase in K_f (Supporting Information Table S-2). At low concentrations, the solute uptake by biochars increases largely with increasing pyrolytic temperature. Linear relationships of N and logK_f values with sorbent's aromaticity (i.e., H/C atomic ratio), or with the pyrolytic temperature, are observed (Supporting Information Figure S-4). Thus, under a given pyrolytic condition, the sorption parameters of a biochar appear to be well related to its pyrolytic temperature; alternatively, the sorption parameters could be used to estimate the charring temperature of a biochar.

Adsorptive Sites and Absorptive Phases of Biochars. Sorption of NOCs to the amorphous domain generates linear isotherms due to partitioning, whereas nonlinear isotherms are observed for a condensed aromatic domain due to a Langmuir-type adsorption or a specific interaction. The pores of black carbon may be shielded by NOM to form BC−NOM complexes (*3, 20*), so that a BC−NOM dual-mode sorption model was used to elucidate the combined adsorption−absorption mechanisms (*20*). Combined adsorption and partition models have been used to assess the contribution of BC to the NOM sorption by soils and sediments and satisfactorily account for the sorptive nonlinearity and the overall sorption (*2, 6, 19, 20*). To characterize the individual roles of BC and NOM, untreated and pretreated samples (by combustion at 375 °C or a chemical extraction method to remove the NOM fraction) are widely used in sorption experiments (*20*). However, the pretreatment significantly would alter the residual fraction's surface properties and medium polarity, and the role of BC in complexes would be significantly magnified by the isolated residues (*3*). This is especially true for biochar samples where the charred fraction (i.e., COM) is derived from its precursor making this approach impractical to study the COM in biochars through a sorbent-pretreatment method. So an isotherm-separation method, as developed for the organobentonite system (*23*), is introduced to quantify respective contribution of adsorption and partition to biochars.

In a mixed adsorption−partition system (e.g., environmental BCs and biochars), the partition effect is favored progressively by increasing the solute concentration, whereas the adsorption contribution reaches saturation more rapidly with the solute concentration (*19*). The isotherm at high concentrations should approach linearity (*6, 19, 23, 24*). This hypothesis is substantiated by the isotherm shape in present and earlier studies (*6, 24, 25*), i.e., being nonlinear at low concentration and linear at high concentrations. Therefore, sorption of NOC to biochar can be defined as

$$Q_T = Q_A + Q_P \quad (1)$$

where Q_T is the total amount of the solute sorbed onto the biochar; Q_A and Q_P are the amounts contributed by adsorption and partition, respectively. Q_A is inclusive of the nonlinear surface coverage and specific interactions, which becomes nearly saturated at low solute concentrations. Q_P includes two dissolution mechanisms, i.e., one with the original amorphous organic matter and the other with the amorphous phase of COM at high solute loading. Hence, Q_P can be calculated as follows,

$$Q_P = K_P C_e \quad (2)$$

Accordingly, at the high solute concentration range the COM and NOM adsorption sites in biochar become saturated and essentially the linear sorption to nonpyrogenic NOM and pyrogenic COM remains. Thus, eq 1 can be transformed to

$$Q_T = Q_A^{max} + Q_P = Q_A^{max} + K_P C_e \quad (3)$$

where Q_A^{max} is the saturated adsorption capacity of a biochar estimated from the high concentration data; $K_P C_e$ is the partition contribution at high concentration with K_P being the partition coefficient; C_e is the solute equilibrium concentration. Linear regression between Q_T and C_e were conducted at high solute concentration range, and the related data are presented in Supporting Information Table S-2. Logically, Q_A^{max} corresponds to the y-axis intercept of the line, and K_P to the slope (see Table 2). The K_P is usually derived

TABLE 2. Partition coefficients and Saturated Adsorption of Organic Pollutants to Bio-chars and an Activated Carbon from Aqueous Solution [a]

	NAPH(2.269)[b]			NB(2.677)[b]			*m*-DNB (1.979)[b]		
sample	K_P/mL·g^{-1}	Q_A^{max}/mg·g^{-1}	$Q_{A,SA}^{max}$/μmol·m^{-2}	K_P/mL·g^{-1}	Q_A^{max}/mg·g^{-1}	$Q_{A,SA}^{max}$/μmol·m^{-2}	K_P/mL·g^{-1}	Q_A^{max}/mg·g^{-1}	$Q_{A,SA}^{max}$/μmol·m^{-2}
P100	295.4	0	0	24.58	0	0	30.99	0	0
P200	782.8	0.329	0.413	72.60	5.908	7.715	88.61	5.655	5.409
P250	783.8	1.724	1.413	94.34	10.08	8.602	99.26	7.535	4.708
P300	785.0	4.006	1.569	129.6	51.14	20.85	109.7	17.09	5.104
P400	748.3	25.69	1.782	71.04	79.71	5.759	66.57	60.01	3.175
P500	299.5	27.40	0.904	29.58	96.63	3.320	25.11	55.23	1.390
P600	274.2	15.14	0.572	19.93	91.99	3.616	0	35.83	1.031
P700	1086	136.8	2.174	85.97	181.2	2.999	70.86	208.0	2.521
AC		314.3	2.366	44.41	386.3	3.028	21.58	424.5	2.437

[a] The slope and *y*-axis intercept of the linear equation (see Supporting Information Table S-2) were used to calculate partition coefficient (K_P) and the maximum adsorption capacity (Q_A^{max}, mg/g, *19, 22*), respectively. $Q_{A,SA}^{max}$ is the SA-normalized Q_A^{max}, i.e., $Q_{A,SA}^{max}$ (μmol·m^{-2}) $= Q_A^{max} \times 1000 \div SA \div M$, where SA is the specific surface area of sorbents, m^2/g; M is the molecular weight of solute, mg/mmol; the number of 1000 is the unit conversion factor. [b] The number in the parentheses is the theoretical estimated value of maximal monolayer arrangement of the tested organic solutes ($Q_{A,mn}^{max}$,μmol·m^{-2}).

via a dual-mode sorption for the partitioning mode in the single-solute experiment, or calculated in the bisolute experiment by applying a competitor at a high concentration to occupy all fixed Langmuir sites so that the second solute could sorb only a partition mode (*25*). Here the Q_A^{max} and K_P values for a heterogeneous sorbent (COM−NOM complexes) may be accurately determined by the isotherm-separation method. Therefore, it becomes more realistic to investigate the correlations of adsorption (Q_A^{max}) with sorbent characteristics (surface and polarity) and sorbate properties (dimension and structure) and the correlations of partition effect (K_P) with the sorbent conformation and polarity.

Based on eqs 1 and 2, the adsorption contribution in the whole isotherm of biochars can be calculated as

$$Q_A = Q_T - Q_P = Q_T - K_P C_e \quad (4)$$

According to eqs 2 and 4, the quantitative contributions of respective partition and adsorption to the total sorption of biochars were calculated, and the selected plots are demonstrated in Figure 3. Reasonably, the separated-adsorption isotherms well fit Langmuir equation (data not shown), and the Q_A reached plateaus (Q_A^{max}). This in turn suggests that the isotherm-separation method is rational to quantify respective contributions of partition and adsorption. The contribution of adsorption increased in the order of P100 < P200 < P250 < P300 < P400 < P600 < P500 < P700, which is in line with their specific SAs. Interestingly, the relative contributions of adsorption and partition vary from P100 to P700 (Supporting Information Figure S-5). The sorption of P100 is dominated absolutely by a partition mechanism for the whole concentration range. For P200 and P250 biochars, COM adsorption sites become saturated at very low concentrations, after which the linear sorption to NOM starts to overwhelm the nonlinear COM contribution (Figure 3(A)). For P300 and P400 samples, the sorption is dominated by adsorption at low to moderate concentration ranges and then overshadowed by partition at high concentrations (Figure 3(B)), while adsorption contribution outweigh the partition effect for P500, P600, and P700 samples at whole concentrations (Figure 3(C)).

The correlations of K_P with sorbent polarity indexes [i.e., (O + N)/C] are shown in Supporting Information Figure S-6. The K_P increase with decreasing polarity indexes of the biochars produced at low pyrolytic temperatures, i.e., P100 < P200 < P250 < P300, reach a maximum with P300, and then decrease with a further decrease of polarity indexes for biochars produced at high pyrolytic temperature, i.e., P300 > P400 > P500 > P600. The major partition phase in P100−P300 is a polymeric aliphatic fraction preserved during the charring process, according to the FTIR data (2927 and 2856 cm^{-1} imply an amorphous state, *26, 27*), and thus the decrease in polarity indexes promotes compatibility of the NOCs with partition phase of biochars. When the pyrolytic temperature over 400 °C, the aliphatic partition phase was eliminated (2927 and 2856 cm^{-1} bands disappeared). Correspondingly, there is a change in the partition medium from a more flexible aliphatic phase to a more rigid and condensed aromatic phase (H/C < 0.451, see Table 1), making the partition less favorable. To our knowledge, this uniquely hyperbolic curves of K_P vs (O + N)/C, relating the partition coefficient to the specific biochar partition phase and polarity, is described for the first time. For P700 samples, at high solute concentrations, the sorbed solute still increases linearly with concentration. This observation cannot be reconciled with partition, because there is presumably little partition phase with P700, judging from its extremely low polarity [(O + N)/C=0.107] and high aromaticity (H/C = 0.176). The K_P value of P700 derived from isotherm-separation method may be attributed to a pore-filling mechanism, as occurs in an activated carbon (*7, 12*). Above C_e = 400 mg/L of NB, the increases of Q values with the order of P100 < P200 < P250 < P500 < P400 < P300 (Figure 2) are attributed to the combined roles of K_P (partition) and Q_A^{max} (adsorption) for each biochar. The K_P values are higher for NAPH than for NB and *m*-DNB to a given biochar mainly due to the former owning strongly hydrophobicity.

The correlations of Q_A^{max} with biochars' SAs are demonstrated in Figure 4. The unit of Q_A^{max} (mg/g) is transformed to μmol/m^2 ($Q_{A,SA}^{max}$, listed in Table 1). The theoretical maximum monolayer capacity ($Q_{A,mn}^{max}$, μmol/m^2) of the NOCs is estimated from the molecular surface area (see Table 1). Based in Table 1 and Figure 4, the adsorptive contributions of P200, P250, P300, and P400 samples, which have a relatively high polarity and an amorphous medium, is dictated by the organic molecular polarity rather than by its dimension. The actual Q_A^{max} values of NB and *m*-DNB (polar molecules) are higher than the predicted values due presumably to additional specific interactions of these polar solutes with polar and amorphous sorbent surfaces (*8, 12, 13, 20*); for NAPH (a nonpolar molecule), the actual Q_A^{max} values are less than predicted because of the interference by adsorbed water in the accessibility of NAPH molecules into polar surface pores (*12*). This effect is better accounted for by a surface polarity-selective effect rather than a porosity-effect. Similar results

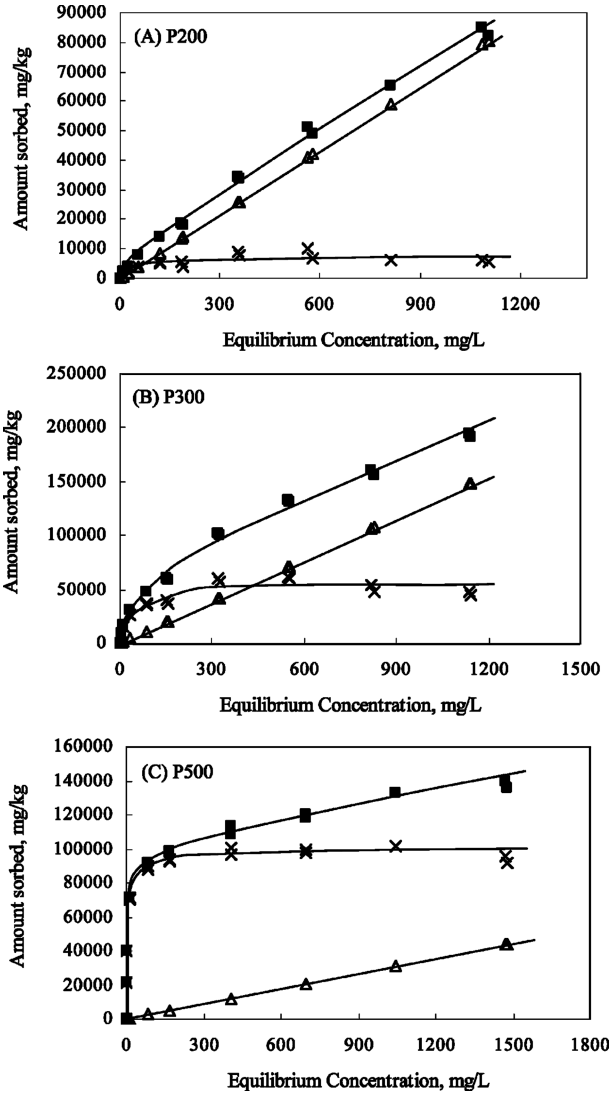

FIGURE 3. Quantitative contributions of partition (Δ) and adsorption (×) to total sorption (■) of nitrobenzene onto the selected biochars (i.e., P200, P300, and P500).

of enhanced sorption of polar NOCs than nonpolar NOCs to wood and crop charcoals were reported (*8, 12*).

Interestingly, for P500 and P600 samples, the relative magnitudes of $Q_{A,SA}^{max}$ (actual) to $Q_{A,mn}^{max}$ (predicted) are dependent on the solute molecular dimension rather than the molecular polarity. For NB with a small size, the experimental Q_A^{max} values are comparable with the theoretical prediction (Figure 4 (B)), whereas the Q_A^{max} values are less than the predicted for large-sized molecules (NAPH and *m*-DNB). The limiting uptake is governed by the accessible micropore volume (i.e., a porosity-effect) rather than by the internal surface area. For P700 biochar and AC, the actual Q_A^{max} values are comparable to the predicted values for the three tested solutes (i.e., NAPH, NB, and *m*-DNB) based on monolayer surface coverage, suggesting that the pores in the P700 and AC are all accessible to these organic molecules, and the surface properties (i.e., the low polarity and highly condensed aromatics) exhibits nonselective effect for different solutes.

The relative magnitudes of maximal adsorptive amounts and theoretical values, shown in Figure 4, clearly demonstrate that there occurs a significant sieving effect which is initially mediated by the size-match between sorbate and biochar's pore (porosity-selective effect), and then by the polar compatibility between sorbate and biochar's surface (polarity-selective effect). The porosity-selective effect dominates

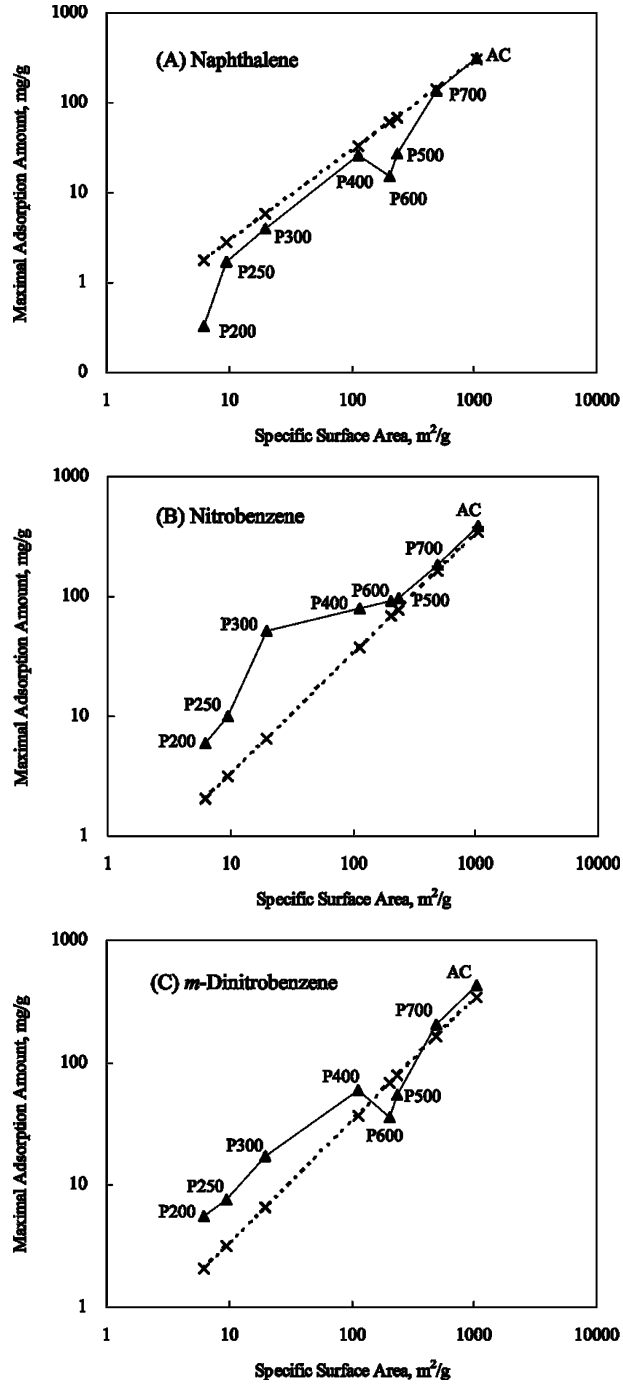

FIGURE 4. Relationships between the adsorptive saturation capacities and the BET-N_2 surface area of sorbents (P200−P700 and AC). ▲ represents the experimental values (Q_A^{max}, mg/g), and × represents the theoretical estimated values from monolayer arrangement of organic molecule.

the adsorption contribution of P500 and P600, which have less surface polarity and pore volume (Table 1). Again, nonselective properties of P700 and AC for the tested solutes may be attributed to its extremely low polar surface (O/C = 0.116 vs 0.175) and a large pore volume (0.186 vs 0.434 mL/g), favoring the accessibility and subsequently the availability to the solutes. These observations can be used to elucidate the jumping sorption of P700 in comparison with P500 and P600. For P700 and AC, the surface coverage (adsorption) may be distinguished from the pore-filling (quasi-partition) uptake by separating partition and adsorption from the total sorption.

In summary, the structures of biochars, significantly altered by the pyrolytic temperature, play an important role in the sorption of various organic contaminants. The quantitative contributions of adsorption and partition are determined by the relative carbonized and noncarbonized fractions and their surface and bulk properties. The observed hyperbolic curves of K_P vs (O + N)/C are related to the specific biochar partition phase and polarity. The partition phase is evolved from an amorphous aliphatic domain to a condensed aromatic core with increasing pyrolytic temperature. The apparent high partition with P700 and AC is attributed to a pore-filling mechanism (a quasi-partition). Simultaneously, the adsorption contribution exhibits a transition from a surface polarity-selective effect to a porosity-selective effect, but displays nonselective effect for P700 and AC in which the experimental Q_A^{max} values are comparable to the theoretical monolayer prediction. The surface polarity-selective effect promotes specific interactions for polar organic solutes, whereas the porosity-selective effect hinders the adsorption of large organic molecules. These observations are crucial to designing the engineered supersorbents (e.g., biochars) and to illustrate the sorption behavior of the COM−NOM complexes.

Acknowledgments

We are highly grateful to the anonymous reviewers and Chiou CT for their valuable comments. This project was supported by the National Natural Science Foundation of China (20577041, 20737002, 40671168), the Program for New Century Excellent Talents in University (NCET-05-0525), and a grant to the author from the National Excellent Doctoral Dissertation of China Foundation (200765).

Supporting Information Available

Properties and dimensions of the selected sorbates in Table S-1 and Figure S-1. Kinetic data, isotherms and their regression parameters in Figure S-2, Figure S-3, and Table S-2. Relationships between logK_f (and N)∼H/C atomic ratio, between K_P∼(O+N)/C), and relative contributions of adsorption and partition in Figure S-4, Figure S-6, and Figure S-5). This material is available free of charge via the Internet at http://pubs.acs.org.

Literature Cited

(1) Cornelissen, G.; Gustafsson, O.; Bucheli, T. D.; Jonker, M. T. O.; Koelmans, A. A.; and Van Noort, P. M. Extensive sorption of organic compounds to black carbon, coal, and kerogen in sediments and soils: mechanisms and consequences for distribution, bioaccumulation, and biodegradation. *Environ. Sci. Technol.* **2005**, *39*, 6881–6895.

(2) Allen-King, R. M.; Grathwohl, P.; Ball, W. P. New modeling paradigms for the sorption of hydrophobic organic chemicals to heterogeneous carbonaceous matter in soils, sediments, and rocks. *Adv. Water Resour.* **2002**, *25*, 985–1016.

(3) Kwon, S.; Pignatello, J. J. Effect of natural organic substances on the surface and adsorptive properties of environmental black carbon (char): Pseudo pore blockage by model lipid components and its implications for N_2-probed surface properties of natural sorbents. *Environ. Sci. Technol.* **2005**, *39*, 7932–7939.

(4) Kuhlbusch, T. A. J. Black carbon and the carbon cycle. *Science* **1998**, *280* (5371), 1903–1904.

(5) Masiello, C. A.; Druffel, E. R. M. Black carbon in deep-sea sediments. *Science* **1998**, *280*, 1911–1913.

(6) Cornelissen, G.; Gustafsson, O. Sorption of phenanthrene to environmental black carbon in sediment with and without organic matter and native sorbates. *Environ. Sci. Technol.* **2004**, *38*, 148–155.

(7) Nguyen, T. H.; Cho, H. H.; Poster, D. L.; Ball, W. P. Evidence for a pore-filling mechanism in the adsorption of aromatic hydrocarbons to a natural wood char. *Environ. Sci. Technol.* **2007**, *41*, 1212–1217.

(8) Sander, M.; Pignatello, J. J. Characterization of charcoal adsorption sites for aromatic compounds: insights drawn from single-solute and bi-solute competitive experiments. *Environ. Sci. Technol.* **2005**, *39*, 1606–1615.

(9) Sheng, G.; Yang, Y. Enhanced pesticide sorption by soils containing particulate matter from crop residue burns. *Environ. Sci. Technol.* **2003**, *37*, 3635–3639.

(10) Pignatello, J. J.; Kwon, S.; Lu, Y. Effect of natural organic substances on the surface and adsorptive properties of environmental black carbon (char): attenuation of surface activity by humic and fulvic acids. *Environ. Sci. Technol.* **2006**, *40*, 7757–7763.

(11) James, G.; Sabatini, D. A.; Chiou, C. T.; Rutherford, D.; Scott, A. C.; Karapanagioti, H. K. Evaluating phenanthrene sorption on various wood chars. *Water Res.* **2005**, *39* (4), 549–558.

(12) Chun, Y.; Sheng, G. Y.; Chiou, C. T.; Xing, B. S. Compositions and sorptive properties of crop residue-derived chars. *Environ. Sci. Technol.* **2004**, *38*, 4649–4655.

(13) Zhu, D. Q.; Kwon, S.; Pignatello, J. J. Adsorption of single-ring organic compounds to wood charcoals prepared under different thermochemical conditions. *Environ. Sci. Technol.* **2005**, *39*, 3990–3998.

(14) Braida, W. J.; Pignatello, J. J.; Lu, Y. F.; Ravikovitch, P. I.; Neimark, A. V.; Xing, B. S. Sorption hysteresis of benzene in charcoal particles. *Environ. Sci. Technol.* **2003**, *37*, 409–417.

(15) Lehmann, J.; Gaunt, J.; and Rondon, M. Bio-char sequestration in terrestrial ecosystems—A review. *Mitigation Adaptation Strategies Global Change* **2006**, *11*, 403–427.

(16) Khlbusch, T. A. J.; Crutzen, P. J. Toward a global estimate of black carbon in residues of vegetation fires representing a sink of atmospheric CO_2 and a source of O_2. *Global Biogeochem. Cycles* **1995**, *9* (4), 491–501.

(17) Renner, R. Rethinking biochar. *Environ. Sci. Technol.* **2007**, *41*, 5932–5933.

(18) Lehmann, J. A handful of carbon. *Nature* **2007**, *447*, 143–144.

(19) Chiou, C. T.; Kile, D. E. Deviations from sorption linearity on soils of polar and nonpolar organic compounds at low relative concentrations. *Environ. Sci. Technol.* **1998**, *32*, 338–343.

(20) Accardi-dey, A.; Gschwend, P. M. Assessing the combined roles of natural organic matter and black carbon as sorbents in sediments. *Environ. Sci. Technol.* **2002**, *36*, 21–29.

(21) Chen, B.; Johnson, E. J.; Chefetz, B.; Zhu, L.; and Xing, B. Sorption of polar and nonpolar aromatic organic contaminants by plant cuticular materials: the role of polarity and accessibility. *Environ. Sci. Technol.* **2005**, *39*, 6138–6146.

(22) Bustin, R. M.; Guo, Y. Abrupt changes (jumps) in reflectance values and chemical compositions of artificial charcoals and inertinite in coals. *Int. J. Coal Geol.* **1999**, *38*, 237–260.

(23) Zhu, L.; Chen, B. Sorption behavior of p-nitrophenol on the interface between anion-cation organobentonite and water. *Environ. Sci. Technol.* **2000**, *34*, 2997–3002.

(24) Nguyen, T. H.; Sabbah, I.; and Ball, W. P. Sorption nonlinearity for organic contaminants with diesel soot: method development and isotherm interpretation. *Environ. Sci. Technol.* **2004**, *38*, 3595–3603.

(25) Graber, E. R.; Sorek, A.; Tsechansky, L.; and Atzomon, N. Competitive uptake of trichloroethene and 1,1,1-trichloroethane byEucalyptus camaldulensis seedlings and wood. *Environ. Sci. Technol.* **2007**, *41*, 6704–6710.

(26) Chen, B.; Li, Y.; Guo, Y.; Zhu, L.; and Schnoor, J. L. Role of the extractable lipids and the polymeric lipids in sorption of organic contaminants onto plant cuticles. *Environ. Sci. Technol.* **2008**, *42*, 1517–1523.

(27) Gefler, M.; Gurger, C.; Fadeev, A.; Sics, I.; Chu, B.; Hsiao, B. S.; Heintz, A.; Kojo, K.; Hsu, S.-L.; Si, M.; Rafailovich, M. Thermally induced phase transitions and morphological changes in organoclays. *Langmuir* **2004**, *30*, 3746–3758.

ES8002684